



# Quantum Control for Nanoscale Spectroscopy With Diamond Nitrogen-Vacancy Centers: A Short Review

Santiago Hernández-Gómez and Nicole Fabbri\*

LENS European Laboratory for Non-linear Spectroscopy, and CNR-INO Istituto Nazionale di Ottica, Sede Secondaria di Sesto Fiorentino, Sesto Fiorentino, Italy

## OPEN ACCESS

### Edited by:

Silvio Sciortino,  
University of Florence, Italy

### Reviewed by:

Dmitry Budker,  
Helmholtz Institute Mainz, Germany  
Muhib Omar,  
Helmholtz Institute Mainz, Germany, in  
collaboration with reviewer DB

Łukasz Ciwiński,  
Institute of Physics, Poland

Jun Tang,  
North University of China, China

### \*Correspondence:

Nicole Fabbri  
fabbri@lens.unifi.it

### Specialty section:

This article was submitted to  
Radiation Detectors and Imaging,  
a section of the journal  
Frontiers in Physics

**Received:** 27 September 2020

**Accepted:** 14 December 2020

**Published:** 10 February 2021

### Citation:

Hernández-Gómez S and Fabbri N  
(2021) Quantum Control for Nanoscale  
Spectroscopy With Diamond  
Nitrogen-Vacancy Centers: A  
Short Review.  
Front. Phys. 8:610868.  
doi: 10.3389/fphy.2020.610868

Diamond quantum technologies based on color centers have rapidly emerged in the most recent years. The nitrogen-vacancy (NV) color center has attracted a particular interest, thanks to its outstanding spin properties and optical addressability. The NV center has been used to realize innovative multimode quantum-enhanced sensors that offer an unprecedented combination of high sensitivity and spatial resolution at room temperature. The technological progress and the widening of potential sensing applications have induced an increasing demand for performance advances of NV quantum sensors. Quantum control plays a key role in responding to this demand. This short review affords an overview on recent advances in quantum control-assisted quantum sensing and spectroscopy of magnetic fields.

**Keywords:** quantum devices, quantum sensors, quantum control, noise spectroscopy, NV centers in diamond

## 1 INTRODUCTION

Optically active point defects in diamond, the so-called color centers, have drawn a general interest in the field of quantum technologies the last few years, thanks to their attractive and variate capabilities [1, 2]. Among diamond color centers, the negatively charged nitrogen-vacancy (NV) center [3, 4] has stood out as a solid-state spin qubit, thanks to a high degree of coherent control, ultra-long spin coherence time, remarkable fluorescence photostability, as well as optical addressability, and initialization and readout, all of which can be achieved at room temperature. The wide range of applications for the NV center includes its use for quantum memories as building blocks of solid-state quantum registers [5, 6], biocompatible quantum sensors [7], and reliable nonclassical sources of single photons [8]. Very recently, NV centers have also been employed as a platform to tackle novel challenges in the investigation of quantum thermodynamics for open systems [9, 10].

As quantum sensors, NV-based sensors exploit quantum resources to enhance the detection of physical signals. They have been successfully used for measuring magnetic and electric fields [11–13], temperature [14, 15], rotation [16], strain and pressure [17], and more. Remarkably, NV magnetometers have been demonstrated to be capable of measuring every localized ultraweak AC fields, achieving sensitivities of the order of  $pT\sqrt{Hz}$  [14] in ambient conditions.

However, as for any other practical device, the operation of NV-based quantum sensor is prone to limitations and imperfections: the high sensitivity to the magnetic environment makes the sensors very precise, but the same interaction with the environment also constitutes a limit to the device sensitivity by reducing the coherence of the quantum states. Along with a progress in the diamond fabrication [18, 19], recent advances in quantum control (QC) offers powerful tools to overcome

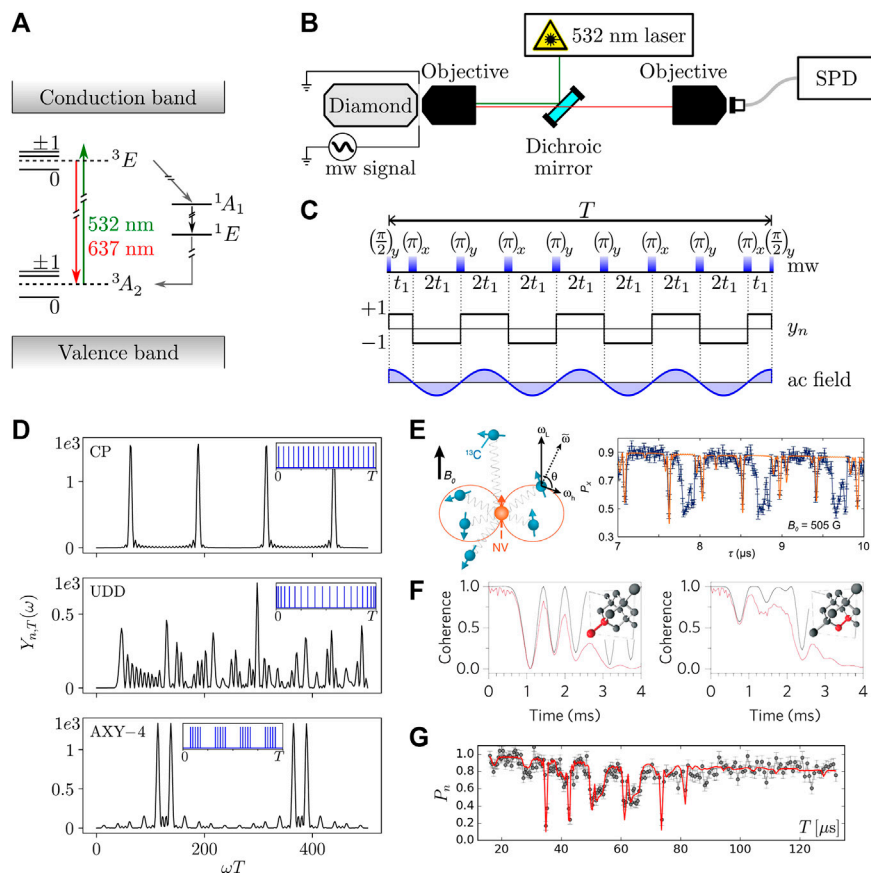


**FIGURE 1 | (A)** Energy level structure of the NV center. **(B)** Simplified scheme of a typical NV experiment implementation. The NV center is addressed with a green laser light via a confocal microscope. The fluorescence emitted by the color center is collected by a single photon detector. An antenna placed in proximity of the diamond chip delivers resonant microwave radiation to control the NV spin dynamics. **(C)** Microwave control pulses distribution of an XY-8 sequence. The qubit acquired phase  $\varphi_n(t)$  is maximized when the filter function  $y_n$  describing the control protocol is synchronized with the target AC field  $b(t)$ . **(D)** Filter function of CP, UDD, and AXY-4 control protocols (see text). Inset: temporal distribution of the  $\pi$  pulses. For simplicity, the number of  $\pi$  pulses is fixed to  $n = 20$ . **(E–G)** NV spin dynamics under DD sequences exemplified in **(D)**. **(E)** Illustrative scheme of the NV center electronic spin and six nearby  $^{13}\text{C}$  nuclear spins. The precession of the nuclear spins depends on their orientation with respect to the NV axis. The right panel shows experimental data relative to the residual population of the  $|1\rangle$  state for a DD protocol using a CP-based sequence with  $n = 32$  equidistant pulses and total sensing time is  $T = 32(2t_1)$ . The orange line represents the prediction after characterizing the interaction with six individual nearby nuclear spins. Adapted from Ref. 68. **(F)** NV spin coherence under a UDD sequence ( $n = 5$ ) in the presence of a  $^{13}\text{C}$  dimer, placed 1.1 nm away from the NV spin (red line), and NV spin coherence once subtracted the effect of the noise-induced decoherence (black line). Each panel refers to a different orientation of the dimer (see inset), with respect to the NV axis. Adapted from Ref. 73. **(G)** Residual population of the  $|1\rangle$  state under an AXY-8 sequence ( $n = 40$ ). The red line shows the predicted dynamics for the interaction with three resolved nuclear spins and with the spin bath. Adapted from Ref. 58.

these limitations. This review study provides a swift compendium of current advances in QC methods and describes how they improve the NV-sensor sensitivity. The content is organized as follows: **Section 2** describes the background of NV magnetometry, with **Section 2.1** introducing the most relevant properties of diamond NV centers, and **Section 2.2** describing basic DC- and AC magnetometry schemes. **Section 2.2** offers an overview on the design of QC protocols for NV center magnetometry and their main applications. Throughout the review, we refer to quantum sensing and spectroscopy schemes that exploit state superpositions as a quantum resource—as opposed to quantum metrology that uses entangled states [20]. Albeit these schemes have been so far mostly employed with single-spin sensing qubits in bulk

diamond [21, 22], they have also emerged as effective tools for nanodiamond-based [23] and ensemble devices [24, 25].

## 2 NV MAGNETOMETRY

### 2.1 The NV Center in Diamond

The NV center is formed by a substitutional nitrogen atom adjacent to a vacancy in the diamond lattice, with  $C_{3v}$  symmetry around one of the four [111] crystallographic directions. In the negatively charged  $\text{NV}^-$ —hereafter referred as NV for simplicity, the favorable internal energy structure and photophysics [4] enable optical initialization and readout and coherent manipulation with long coherence

time, opening the way for many quantum technology applications.

The NV energy structure, shown in **Figure 1A**, consists of electronic orbital ground ( ${}^3A_2$ ) and excited ( ${}^3E$ ) triplet levels separated by 1.945 eV and two intermediate  ${}^1E$  and  ${}^1A_1$  singlet levels [4]. Within the spin-1 triplet ground state, the spin projection  $m_s = 0$  is separated from the degenerate  $m_s = \pm 1$  owing to the electronic spin–spin interaction within the NV, with zero-field splitting of  $D_g \approx 2.87$  GHz. A static bias magnetic field further splits the levels  $m_s = \pm 1$  and modifies their energies *via* the Zeeman effect. A microwave excitation can be used to selectively address one of the  $m_s = 0 \rightarrow \pm 1$  transitions. Thus, the NV center at room temperature can be effectively employed as a single-qubit probe system, with  $|0\rangle$  and  $|1\rangle$  being a pair of spin projections. The success of this platform is primarily due to its remarkably long spin coherence time compared to any other solid-state platform. In most of NV implementations, dephasing is induced by the slowly varying inhomogeneity of the dipolar fields due to unpolarized spin impurities ( ${}^{13}\text{C}$  and  ${}^{14}\text{N}$ ) within the diamond crystal. In type II-a CVD-grown bulk diamond with carbon natural abundance operated at room temperature, the dominant contribution is due to the coupling with a  ${}^{13}\text{C}$  nuclear spin bath with characteristic time  $T_2^* \sim \mu\text{s}$  [24], while in isotopically purified diamond  $T_2^*$  reaches  $\sim 100 \mu\text{s}$  [11]. Dephasing can be mitigated *via* dynamical decoupling, attaining coherence times typically limited by  $T_2 \sim 0.5T_1$ , with longitudinal relaxation times  $T_1 \sim 6$  ms at room temperature and  $T_1 \sim 1$  s at cryogenic temperature ( $T = 77$  K) [22, 26]. At room temperature, the triplet ground-state population—distributed according to Maxwell–Boltzmann distribution—can be transferred to the excited levels by irradiation of the center with green laser light (532 nm) through a process involving a combination of radiative absorption and non-radiative relaxation processes that also entail vibronic bands. A direct spin-preserving radiative decay from the excited to the ground level (with zero-phonon line of 637-nm wavelength) is accompanied by non-radiative non-spin-preserving decay through the long-lifetime singlet levels  ${}^1A_1$  and  ${}^1E$ . The different decay rates for the different spin projections in the non-radiative decay channel yield the optical initialization of the system into the  $m_s = 0$  state of the ground level. The same decay mechanism enables spin state readout, thanks to different photoluminescence intensities of the  $m_s = 0$  and  $m_s = \pm 1$  states. A simplified sketch of a typical experimental setup for NV control is in **Figure 1B**.

## 2.2 Magnetic Field Sensing

Among sensing applications of NV centers, magnetometry—that is, the measurement of magnetic field strength and orientation—has received by far the most attention. As also for magnetometers based on gaseous alkali atoms, all the sensing protocols of NV magnetometers essentially reside within the measurement of the Zeeman splitting induced by an external magnetic field. The most basic scheme consists in the direct measurement of the transition frequency  $|0\rangle \rightarrow |1\rangle$ , *via* optically detected electron spin resonance (ESR). This method has enabled the measurement of DC magnetic field, including, for example, mapping of magnetic distributions with scanning probe

magnetometers [27], magnetic imaging in living cells with sub-cellular spatial resolution [28], and noninvasive detection of action potentials with single-neuron sensitivity [29]. This method is inherently limited to magnetic fields with amplitude and orientation such that the spin quantization axis remains aligned with the NV symmetry axis: since the NV readout relies on spin-dependent photoluminescence intensity, the spin mixing induced by orthogonal components of the magnetic field reduces the contrast of optically detected ESR [30]. However, the concomitant decrease of photoluminescence observed in the presence of any off-axis field has been used to perform all-optical magnetic field mapping [30]. Vectorial magnetometry is possible with NV ensembles by exploiting the four different possible orientations of the NV centers in the diamond crystal [31, 32].

For advanced sensing applications, a more precise determination of the transition frequency can be achieved with interferometric techniques. The basis of these techniques is Ramsey interference [33], where the spin is prepared in a superposition state  $|0\rangle + e^{i\varphi_0}|1\rangle$ , and the spin phase  $\varphi$  accumulated during the interrogation time reflects the addressed transition frequency, which depends on the external field to be measured. The Ramsey scheme is sensitive to static, slowly varying, or broadband near-DC signals [20]. The sensitivity achieved with DC magnetometry schemes is limited by the dephasing time  $T_2^*$ .

Higher sensitivity can be attained when measuring AC magnetic fields, by implementing a dynamical decoupling (DD) of the NV spin from its environment, thus prolonging the NV coherence time. The elementary DD protocol is Hahn's echo, where a  $\pi$  pulse applied halfway of the spin precession time reverses the spin evolution, so that the phase accumulated in the two time segments cancels out. This concept can be extended to multiple refocusing  $\pi$  pulses, as shown in the next Section. The bandwidth of DD protocols usually extends up to  $\sim 10$  MHz [34–36], although interesting sensing schemes for signal detection up to  $\sim 100$  MHz [37] and even GHz [38] have also been proposed. AC sensitivity is limited by the coherence time (also referred to as transverse relaxation time)  $T_2$ —due to homogeneous fluctuating fields, which can exceed  $T_2^*$  by two orders of magnitude [21].

## 3 MAGNETIC SPECTROSCOPY

The resonant driving techniques developed for nuclear magnetic resonance (NMR) Ref. 39 in the first part of the previous century are still relevant for the development of novel techniques [3]. In this section, we explore some recent proposals that have taken NV magnetometry to new limits, focusing on pulsed DD protocols.

The spectral characterization of a magnetic field can be conducted through the analysis of relaxation and dephasing processes occurring to the probe system itself due to the interaction with the target field. Relaxometry consists in the measurement of the relaxation rate  $\Gamma$  of the sensor that is connected with the spectral density of a signal  $S(\omega)$ , linearly in

the first-order approximation. This method—introduced in NMR [40] and also applied to superconductive qubits [41–44]—has been exploited with NV sensors to investigate especially high-frequency noise, through on the measurements of the  $T_1$  relaxation time [35, 45–49].

The alternative approach relies on the systematic analysis of the sensor decoherence under a set of DD control protocols [50–56]. Pulsed DD protocols, based on the Hahn’s spin echo sequence, consist in sequences of  $\pi$  pulses that repeatedly flip the qubit spin, hence reversing its evolution, as sketched in **Figure 1C**: they realize narrow frequency filters that select only a specific coupling and frequency to be probed, while decoupling the sensor from the rest of the environment, hence extending the coherence time of the qubit to increase the measurement precision [20].

In several NV implementations, dephasing can be modeled as due to a classical stochastic noise source [57, 58]. In the presence of pure classical dephasing [55, 59, 60], the DD control protocols can be effectively captured by the filter function approach [20]. The control field can be described by a modulation function  $y_n(t)$  with a sign switch at the position of each  $\pi$  pulse, indicating the direction of time evolution, forward or backward. The NV spin phase  $\phi$  acquired during the sensing time  $T$  is mapped into the residual population of the state  $|1\rangle$ :

$$P(T) = \frac{1}{2} (1 + W(T)), \tag{1}$$

where  $W$  is the qubit coherence. Since the source of dephasing is the nuclear spin bath that couples weakly to external magnetic target fields due the small nuclear magnetic moment, the qubit coherence  $W$  can be factorized in two contributions due to the external field to be measured  $W^{(ac)}$  and to the noise  $W^{(NSD)}$ . In the presence of a target AC magnetic field  $b(t) \equiv bf(t)$ , the phase acquired under the action of the control field,  $\phi = \int_0^T \gamma b(t) y_n(t) dt$ , modulates the qubit coherence as  $W^{(ac)}(T) = \cos\phi(T)$ . On the other hand, the interaction with a detrimental noise source, with an associated noise spectral density (NSD)  $S(\omega)$ , tends to destroy the qubit coherence  $W^{(NSD)}(T) = e^{-\chi_n(T)}$ , where the decoherence function  $\chi_n(T) = \int \frac{d\omega}{\pi\omega^2} S(\omega) |Y_{n,T}(\omega)|^2$  [51, 58, 59] is the convolution between the NSD and the filter function  $Y_{n,T}(\omega) = 1 + (-1)^{n+1} e^{-i\omega T} + 2 \sum_{j=1}^n (-1)^j e^{-i\omega\delta_j}$ , where  $\delta_j$  is the position of the  $j$ th  $\pi$  pulse<sup>1</sup> (see **Figure 1D**). For a single-spin sensor, sensitivity—that is, the minimum detectable signal per unit time—can be quantified as [20, 61]

$$\eta = \frac{e^{\chi_n(T)}}{|\phi(T)|} \sqrt{T}, \tag{2}$$

<sup>1</sup>Note that  $S(\omega)$  is expressed in MHz, and  $Y_{n,T}(\omega)$  is dimensionless. An alternative formulation of the filter function is reported in Ref. 20, where  $\chi_n(T) = 1/\pi \int d\omega S(\omega) |\mathcal{Y}_{n,T}(\omega)|^2$  with a filter function  $\mathcal{Y}_{n,T}(\omega) \equiv \int_0^T dt e^{-i\omega t} y_n(t)$  expressed in units of 1/Hz.

**TABLE 1** | Filter function  $Y_{n,T}(\omega)$  of ESR, Ramsey free induction decay (FID), and selected pulsed DD protocols [20, 51].  $n$ , the total number of pulses;  $T$ , the sensing time;  $t_\pi$ , the pulse length;  $c$ , a normalization constant. For nested sequences,  $N$  is the number of repetitions of a  $M$ -pulse block; the position in time of each pulse is  $t_{m,n} = [(2n-1)/2 + r_m](T/N)$  with  $n = 1, 2, \dots, N$  and  $m = 1, 2, \dots, M$

Protocol	$ Y_{n,T}(\omega) ^2$	Reference
ESR	$\begin{cases} 1/c, & \text{for } 2\pi/T < \omega < t_\pi \\ 0, & \text{otherwise} \end{cases}$	[77]
FID	$2\sin^2(\omega T/2)$	[20]
CP (even $n$ )	$8[\sec(\omega T/2n)\sin(\omega T/2)\sin^2(\omega T/4n)]^2$	[62]
UDD	$\frac{1}{2} \left  \sum_{k=-n-1}^n (-1)^k \exp\left[\frac{i\omega T}{2} \cos\left(\frac{\pi k}{n+1}\right)\right] \right ^2$	[72]
Nested sequence <sup>a</sup>	$16 \frac{\sin^2(\omega T/2)}{\cos^2(\omega T/2N)} [\cos^2(\omega T/4N) - \cos(r\omega T/N)]^2$	[74]

<sup>a</sup>For  $M = 3$ ,  $r_2 = 0$  and  $r_3 = -r_1 \equiv r$  with  $r \in \left[-\frac{1}{2}, \frac{1}{2}\right]$

where  $\phi = \phi/b$  is the acquired phase per unit field. Effective sensing thus relies on the identification of the optimal filter function that minimizes sensitivity, requiring the twofold tasks of capturing the target signal and rejecting unwanted noise, which may be even conflicting when signal and noise have mutual spectral content. Huge effort has been devoted in the last years to develop a suite of DD-based spin manipulation protocols, opportunely tailored for mitigating the effect of different noise sources of decoherence, optimizing the decoupling performance, narrowing the spectral response and suppressing signal harmonics and sidebands, as well as compensating pulse errors [51].

A large family of DD protocols is constituted by periodically structured train of pulses. An example is the Carr–Purcell (CP) sequence [62], formed by  $n$  equidistant  $\pi$  pulses, which enables the detection of monochromatic AC fields with periodicity commensurate with the interpulse delay time  $2t_i$ : this pulse train acts as a narrow quasi-monochromatic and tunable filter, where  $t_i$  selects the pass-band frequency, while  $n$  determines the filter width [63, 64]. As an extension of this scheme, XY-N sequences [65] are designed to improve robustness against detuning and imperfections of the  $\pi$  pulses, by symmetrically rotating their relative phase (see **Figure 1C**). Periodic protocols have been demonstrated to be ideal for decoupling from environments with soft frequency cutoff, such as P1 centers electronic spin bath [21, 23, 66]. They have been exploited in NV sensor settings to detect and characterize individual <sup>13</sup>C nuclear spins [67–69], demonstrating the possibility of sensing single nuclear spins placed a few nanometers apart from the NV center (see **Figure 1E**) and to detect and characterize proton spins of molecules in organic samples placed some nanometers outside the diamond [70, 71].

Further developments are introduced by non-equispaced and concatenated sequences. The Uhrig DD (UDD) protocol [72], composed by a set of  $n$   $\pi$ -pulses with interpulse delay time  $\delta_j = \sin^2[\pi j/(2n+2)]$  and  $j \in \{1, \dots, n\}$ , has been successfully employed to detect <sup>13</sup>C dimers [73] inside the diamond as it highly suppresses the effect of coupling to single nearby nuclei (see **Figure 1F**). Nested sequences composed by repeated blocks of periodic or aperiodic  $\pi$  pulses were designed to facilitate the discrimination of single nuclear spins [74], thanks to high-frequency selectivity and moderate peak strength of the filter

function. Adding phase rotation within each block improves the robustness against pulse errors, an example of which being the adaptive XY-N (AXY-N) sequence [75], where each block is a Knill pulse formed by  $M = 5$  equidistant  $\pi$  pulses [75, 76] (see **Figure 1G**). The analytic expressions of the filter functions of the mentioned protocols are reported in **Table 1**.

The search for optimized DD protocols has also benefited from the application of quantum optimal control (QOC) theory [78, 79], which exploits numerical optimization methods to find the best control field that opportunely steers the system dynamics toward a desired objective, subject to some control restrictions determined by physical and experimental constraints. In the very last years, QOC has shown a number of interesting results on NV settings [61, 80–83]. By introducing the Fisher information of the measurement as the cost function of the optimization [61], QOC can naturally take into account both the signal of interest and the environmental noise to find the optimal DD spin manipulation protocol (e.g., defining the optimal pulse distribution). QOC-DD schemes have been successfully employed in single-qubit sensing of complex AC fields, demonstrating a significant sensitivity improvement compared to the CP scheme [61].

### 3.1 Noise Spectroscopy

A good knowledge of the environment is imperative in order to improve the sensor capabilities, either by allowing to strategically filter out the unwanted noise components [84], or by using part of the environment as ancillary systems [85].

In type-IIa diamond, the carbon nuclear spin environment can be divided into a small set of strongly coupled nuclei and a large nuclear spin bath. The coherent coupling with the resolved nuclei can be characterized, as mentioned before, using periodic DD sequences [67–69]. On the other hand, the interaction with the collective bath is responsible for the NV decoherence and its description is more involved. In the presence of strong bias magnetic field, the environment internal energy overcomes the typical NV-bath coupling strength. In this weak-coupling regime, the spin bath can be modeled as a classical stochastic field with NSD peaked at the  $^{13}\text{C}$  Larmor frequency [55, 58]. However, the spectral characterization of noise can be quite challenging, and requires deconvolution analysis. The most common approach involves using CP-based sequences with large  $n$ , resulting in a filter function that can be approximated to a Dirac comb. Measuring a generalized coherence time [54, 55] allows the reconstruction of the NSD lineshape. When the noise is strong enough to destroy coherence in short times, using higher harmonics of the filter function for the NSD characterization will give cleaner and more accurate results [58, 86]. For low bias fields ( $\leq 150$  G), the loss of NV coherence is due to the creation of entanglement between NV spin and the large environment: In this strong-coupling regime, the environment description in terms of classic noise is no longer valid [57], and the dynamics of the nuclear spin environment itself is affected by the control applied to the NV center electronic spin, due to the NV back action [58].

In isotopically purified samples, paramagnetic impurities—especially P1 centers—dominate the NV dephasing. This

electronic spin bath has been characterized with single-spin sensors and ensembles by combining either Hanh echo [23] or double quantum coherence magnetometry that employs the  $m_s = \{+1, -1\}$  NV spin ground-state subspace [87], with radiofrequency bath driving [88].

## 4 SUMMARY AND PROSPECT

Diamond NV centers have been established as a prominent platform for a suite of quantum technology applications, among which quantum sensing is definitely the most mature. Quantum control plays a crucial role in improving the sensor performance, by enhancing the sensor response to the target field to be measured, while protecting it against the remaining environment. Among QC strategies, the development of multi-pulse DD protocols for the NV spin manipulation has opened the way to impressive progress in magnetic spectroscopy, making possible the detection of ultrathin magnetic fields such as that originated by single nuclei in the proximity of the NV sensor.

DD techniques have been so far mainly employed for single isolated sensing qubits in bulk diamond. Major challenges and potential breakthroughs currently concern the application of DD spin manipulation protocols to two other relevant classes of NV magnetometers: scanning probe magnetometers—which guarantee the best performance in terms of spatial resolution by virtue of the use of nano-fabricated diamond tips, and ensemble magnetometers—providing enhanced signal-to-noise ratio thanks to the statistical averaging over multiple spins. Albeit DD protocols have been demonstrated to be beneficial in multispin metrology [24, 25] and in high-purity nanodiamonds [23], often the poor spin coherence properties of NV-rich bulk diamond and nanodiamond NVs have so far limited the application of these classes of settings to the measurement of strong DC fields based on optically detected ESR or Ramsey interferometry, where sensitivity is limited by the dephasing time  $T_2^*$ , presently far away by orders of magnitude from the physical limit of  $T_1/2$ . This hindrance is not fundamental and will be presumably overcome in the near future *via* improved synthesis techniques [89], convenient experimental design (e.g., magnetic gradient compensation and operation under strong bias magnetic fields to mitigate the effect of external electric field gradients and internal strain) [90], as well as increased collection efficiency [91]. The application of DD spin manipulation protocols to scanning NV magnetometers and ensemble devices could pave the way to reach fundamental metrology limits and dramatically expand the range of envisioned nanoscale applications, for example, enabling the detection of arbitrary individual spins in ensembles in the presence of environmental noise.

## AUTHOR CONTRIBUTIONS

SH and NF wrote this review article and they are responsible for the content of the work.

## REFERENCES

- Bradac C, Gao W, Forneris J, Trusheim ME, Aharonovich I. Quantum nanophotonics with group IV defects in diamond. *Nat Commun* (2020) 1–13. doi:10.1038/s41467-019-13332-w
- Thiering G, Gali A. Color centers in diamond for quantum applications. *Diamond Quant Appl* (2020) 103:1–36. doi:10.1016/bs.semsem.2020.03.001
- Dobrovitski V, Fuchs G, Falk A, Santori C, Awschalom D. Quantum control over single spins in diamond. *Ann Rev Condens Matter Phys* (2013) 4:23–50. doi:10.1146/annurev-conmatphys-030212-184238
- Doherty MW, Manson NB, Delaney P, Jelezko F, Wrachtrup J, Hollenberg LC. The nitrogen-vacancy colour centre in diamond. *Phys Rep* (2013) 528:1–45. doi:10.1016/j.physrep.2013.02.001
- Neumann P, Mizuochi N, Rempp F, Hemmer P, Watanabe H, Yamasaki S, et al. Multipartite entanglement among single spins in diamond. *Science* (2008) 320:1326–9. doi:10.1126/science.1157233
- Bradley CE, Randall J, Aboeih MH, Berrevoets RC, Degen MJ, Bakker MA, et al. A ten-qubit solid-state spin register with quantum memory up to one minute. *Phys Rev X* (2019) 9:031045. doi:10.1103/PhysRevX.9.031045
- Rondin L, Tetienne JP, Hingant T, Roch JF, Maletinsky P, Jacques V. Magnetometry with nitrogen-vacancy defects in diamond. *Rep Prog Phys* (2014) 77:056503–27. doi:10.1088/0034-4885/77/5/056503
- Sipahigil A, Goldman ML, Togan E, Chu Y, Markham M, Twitchen DJ, et al. Quantum interference of single photons from remote nitrogen-vacancy centers in diamond. *Phys Rev Lett* (2012) 108:143601. doi:10.1103/PhysRevLett.108.143601
- Klatzow J, Becker JN, Ledingham PM, Weinzel C, Kaczmarek KT, Saunders DJ, et al. Experimental demonstration of quantum effects in the operation of microscopic heat engines. *Phys Rev Lett* (2019) 122:110601. doi:10.1103/physrevlett.122.110601
- Hernández-Gómez S, Gherardini S, Poggiali F, Cataliotti FS, Trombettoni A, Cappellaro P, et al. Experimental test of exchange fluctuation relations in an open quantum system. *Phys Rev Res* (2020) 2:023327. doi:10.1103/PhysRevResearch.2.023327
- Balasubramanian G, Neumann P, Twitchen D, Markham M, Kolesov R, Mizuochi N, et al. Ultralong spin coherence time in isotopically engineered diamond. *Nat Mater* (2009) 8:383–7. doi:10.1038/nmat2420
- Wolf T, Neumann P, Nakamura K, Sumiya H, Ohshima T, Isoya J, et al. Subpicotesla diamond magnetometry. *Phys Rev X* (2015) 5:041001. doi:10.1103/PhysRevX.5.041001
- Dolde F, Fedder H, Doherty MW, Nöbauer T, Rempp F, Balasubramanian G, et al. Electric-field sensing using single diamond spins. *Nat Phys* (2011) 7:459–63. doi:10.1038/nphys1969
- Acosta VM, Bauch E, Ledbetter MP, Waxman A, Bouchard LS, Budker D. Temperature dependence of the nitrogen-vacancy magnetic resonance in diamond. *Phys Rev Lett* (2010) 104:070801. doi:10.1103/PhysRevLett.104.070801
- Neumann P, Jakobi I, Dolde F, Burk C, Reuter R, Waldherr G, et al. High-precision nanoscale temperature sensing using single defects in diamond. *Nano Lett* (2013) 13:2738–42. doi:10.1021/nl401216y
- Soshenko VV, Bolshedvorskii SV, Rubinas O, Sorokin VN, Smolyaninov AN, Vorobyov VV, et al. Nuclear spin gyroscope based on the nv center in diamond. arXiv:2009.00916 (2020).
- Teissier J, Barfuss A, Appel P, Neu E, Maletinsky P. Strain coupling of a nitrogen-vacancy center spin to a diamond mechanical oscillator. *Phys Rev Lett* (2014) 113:020503. doi:10.1103/PhysRevLett.113.020503
- Markham ML, Dodson JM, Scarsbrook GA, Twitchen DJ, Balasubramanian G, Jelezko F, et al. CVD diamond for spintronics. *Diam Relat Mater* (2011) 20:134–9. doi:10.1016/j.diamond.2010.11.016
- Waldermann FC, Olivero P, Nunn J, Surmacz K, Wang ZY, Jaksch D, et al. Creating diamond color centers for quantum optical applications. *Diam Relat Mater* (2007) 16:1887–95. doi:10.1016/j.diamond.2007.09.009
- Degen CL, Reinhard F, Cappellaro P. Quantum sensing. *Rev Mod Phys* (2017) 89:035002. doi:10.1103/RevModPhys.89.035002
- de Lange G, Wang ZH, Riste D, Dobrovitski VV, Hanson R. Universal dynamical decoupling of a single solid-state spin from a spin bath. *Science* (2010) 330:60–3. doi:10.1126/science.1192739
- Bar-Gill N, Pham L, Jarmola A, Budker D, Walsworth R. Solid-state electronic spin coherence time approaching one second. *Nat Commun* (2013) 4:1743. doi:10.1038/ncomms2771
- Knowles HS, Kara DM, Atature M. Observing bulk diamond spin coherence in high-purity nanodiamonds. *Nat Mater* (2014) 13, 21–5. doi:10.1038/nmat3805
- Pham LM, Bar-Gill N, Belthangady C, Le Sage D, Cappellaro P, Lukin MD, et al. Enhanced solid-state multispin metrology using dynamical decoupling. *Phys Rev B* (2012) 86:045214. doi:10.1103/PhysRevB.86.045214
- Bar-Gill N, Pham L, Belthangady C, Le Sage D, Cappellaro P, Maze J, et al. Suppression of spin-bath dynamics for improved coherence of multi-spin-qubit systems. *Nat Commun* (2012) 3:858. doi:10.1038/ncomms1856
- Jarmola A, Acosta VM, Jensen K, Chemerisov S, Budker D. Temperature- and magnetic-field-dependent longitudinal spin relaxation in nitrogen-vacancy ensembles in diamond. *Phys Rev Lett* (2012) 108:197601. doi:10.1103/PhysRevLett.108.197601
- Rondin L, Tetienne JP, Rohart S, Thiaville A, Hingant T, Spinicelli P, et al. Stray-field imaging of magnetic vortices with a single diamond spin. *Nat Commun* (2013) 4:2279. doi:10.1038/ncomms3279
- Le Sage D, Arai K, Glenn DR, DeVience SJ, Pham LM, Rahn-Lee L, et al. Optical magnetic imaging of living cells. *Nature* (2013) 496:486–9. doi:10.1038/nature12072
- Barry JF, Turner MJ, Schloss JM, Glenn DR, Song Y, Lukin MD, et al. Optical magnetic detection of single-neuron action potentials using quantum defects in diamond. *Proc Natl Acad Sci USA* (2016) 113:14133–8. doi:10.1073/pnas.1601513113
- Tetienne JP, Rondin L, Spinicelli P, Chipaux M, Debuisschert T, Roch JF, et al. Magnetic-field-dependent photodynamics of single nv defects in diamond: an application to qualitative all-optical magnetic imaging. *New J Phys* (2012) 14:103033. doi:10.1088/1367-2630/14/10/103033
- Maert BJ, Wijnheijmer AP, Fuchs GD, Nowakowski ME, Awschalom DD. Vector magnetic field microscopy using nitrogen vacancy centers in diamond. *Appl Phys Lett* (2010) 96:092504. doi:10.1063/1.3337096
- Pham LM, Le Sage D, Stanwix PL, Yeung TK, Glenn D, Trifonov A, et al. Magnetic field imaging with nitrogen-vacancy ensembles. *New J Phys* (2011) 13:045021. doi:10.1088/1367-2630/13/4/045021
- Ramsey NF. A molecular beam resonance method with separated oscillating fields. *Phys Rev* (1950) 78:695–9. doi:10.1103/PhysRev.78.695
- Laraoui A, Hodges JS, Meriles CA. Magnetometry of random ac magnetic fields using a single nitrogen-vacancy center. *Appl Phys Lett* (2010) 97:143104. doi:10.1063/1.3497004
- Steinert S, Ziem F, Hall LT, Zappe A, Schweikert M, Gutz N, et al. Magnetic spin imaging under ambient conditions with sub-cellular resolution. *Nat Commun* (2013) 4:1607. doi:10.1038/ncomms2588
- Schmitt S, Gefen T, Stürner F, Uden T, Wolff G, Müller C, et al. Submillihertz magnetic spectroscopy performed with a nanoscale quantum sensor. *Science* (2017) 356:832–7. doi:10.1126/science.aam5532
- Aslam N, Pfender M, Neumann P, Reuter R, Zappe A, Fávora de Oliveira F, et al. Nanoscale nuclear magnetic resonance with chemical resolution. *Science* (2017) eaam8697. doi:10.1126/science.aam8697
- Joas T, Waerber AM, Braunbeck G, Reinhard F. Quantum sensing of weak radio-frequency signals by pulsed Mollow absorption spectroscopy. *Nat Commun* (2017) 8:964. doi:10.1038/s41467-017-01158-3
- Abraham A. *Principles of nuclear magnetism*. Oxford, UK: Oxford University Press (1961).
- Kimmich R, Anardo E. Field-cycling nmr relaxometry. *Prog Nucl Magn Reson Spectrosc* (2004) 44:257. doi:10.1038/nature07127
- Bialczak RC, McDermott R, Ansmann M, Hofheinz M, Katz N, Lucero E, et al. Flux noise in josephson phase qubits. *Phys Rev Lett* (2007) 99:187006. doi:10.1103/PhysRevLett.99.187006
- Lanting T, Berkley AJ, Bumble B, Bunyk P, Fung A, Johansson J, et al. Geometrical dependence of the low-frequency noise in superconducting flux qubits. *Phys Rev B* (2009) 79:060509. doi:10.1103/PhysRevB.79.060509
- Bylander J, Gustavsson S, Yan F, Yoshihara F, Harrabi K, Fitch G, et al. Noise spectroscopy through dynamical decoupling with a superconducting flux qubit. *Nat Phys* (2011) 7:565–70. doi:10.1038/nphys1994
- Yan F, Gustavsson S, Bylander J, Jin X, Yoshihara F, Cory DG, et al. Rotating-frame relaxation as a noise spectrum analyser of a superconducting qubit

- undergoing driven evolution. *Nat Commun* (2013) 4:2337. doi:10.1038/ncomms3337
45. Myers BA, Das A, Dartiailh MC, Ohno K, Awschalom DD, Jayich ACB. Probing surface noise with depth-calibrated spins in diamond. *Phys Rev Lett* (2014) 113:027602. doi:10.1103/physrevLetters113.027602
  46. Rosskopf T, Dussaux A, Ohashi K, Loretz M, Schirhagl R, Watanabe H, et al. Investigation of surface magnetic noise by shallow spins in diamond. *Phys Rev Lett* (2014) 112:147602. doi:10.1103/PhysRevLetters112.147602
  47. van der Sar T, Casola F, Walsworth R, Yacoby A. Nanometre-scale probing of spin waves using single electron spins. *Nat Commun* (2015) 6:7886. doi:10.1038/ncomms8886
  48. Romach Y, Müller C, Unden T, Rogers LJ, Isoda T, Itoh KM, et al. Spectroscopy of surface-induced noise using shallow spins in diamond. *Phys Rev Lett* (2015) 114:017601. doi:10.1103/PhysRevLetters114.017601
  49. Stark A, Aharon N, Unden T, Louzon D, Huck A, Retzker A, et al. Narrow-bandwidth sensing of high-frequency fields with continuous dynamical decoupling. *Nat Commun* (2018) 8:1105. doi:10.1038/s41467-017-01159-2
  50. Viola L, Lloyd S. Dynamical suppression of decoherence in two-state quantum systems. *Phys Rev* (1998) 58:2733. doi:10.1103/PhysRevA.58.2733
  51. Cywiński L, Lutchyn RM, Nave CP, DasSarma S. How to enhance dephasing time in superconducting qubits. *Phys Rev B* (2008) 77:174509. doi:10.1103/PhysRevB.77.174509
  52. Faoro L, Viola L. Dynamical suppression of noise processes in qubit systems. *Phys Rev Lett* (2004) 92:117905. doi:10.1103/PhysRevLetters92.117905
  53. Almog I, Sagi Y, Gordon G, Bensky G, Kurizki G, Davidson N. Direct measurement of the system-environment coupling as a tool for understanding decoherence and dynamical decoupling. *J Phys B Atom Mol Opt Phys* (2011) 44:154006. doi:10.1088/0953-4075/44/15/154006
  54. Yuge T, Sasaki S, Hirayama Y. Measurement of the noise spectrum using a multiple-pulse sequence. *Phys Rev Lett* (2011) 107:170504. doi:10.1103/PhysRevLetters107.170504
  55. Álvarez GA, Suter D. Measuring the spectrum of colored noise by dynamical decoupling. *Phys Rev Lett* (2011) 107:230501. doi:10.1103/PhysRevLetters107.230501
  56. Young KC, Whaley KB. Qubits as spectrometers of dephasing noise. *Phys Rev* (2012) 86:012314. doi:10.1103/PhysRevA.86.012314
  57. Reinhard F, Shi F, Zhao N, Rempp F, Naydenov B, Meijer J, et al. Tuning a spin bath through the quantum-classical transition. *Phys Rev Lett* (2012) 108:200402. doi:10.1103/PhysRevLetters108.200402
  58. Hernández-Gómez S, Poggiali F, Cappellaro P, Fabbri N. Noise spectroscopy of a quantum-classical environment with a diamond qubit. *Phys Rev B* (2018) 98:214307. doi:10.1103/PhysRevB.98.214307
  59. Biercuk MJ, Doherty AC, Uys H. Dynamical decoupling sequence construction as a filter-design problem. *J Phys B* (2011) 44:154002. doi:10.1088/0953-4075/44/15/154002
  60. Kotler S, Akerman N, Glickman Y, Keselman A, Ozeri R. Single-ion quantum lock-in amplifier. *Nature* (2011) 473:61–5. doi:10.1038/nature10010
  61. Poggiali F, Cappellaro P, Fabbri N. Optimal control for one-qubit quantum sensing. *Phys Rev X* (2018) 8:021059. doi:10.1103/PhysRevX.8.021059
  62. Carr HY, Purcell EM. Effects of diffusion on free precession in nuclear magnetic resonance experiments. *Phys Rev* (1954) 94:630–8. doi:10.1103/PhysRev.94.630
  63. Taylor JM, Cappellaro P, Childress L, Jiang L, Budker D, Hemmer PR, et al. High-sensitivity diamond magnetometer with nanoscale resolution. *Nat Phys* (2008) 4:810–6. doi:10.1038/nphys1075
  64. Maze JR, Stanwix PL, Hodges JS, Hong S, Taylor JM, Cappellaro P, et al. Nanoscale magnetic sensing with an individual electronic spin qubit in diamond. *Nature* (2008) 455:644–7. doi:10.1038/nature07279
  65. Gullion T, Baker DB, Conradi MS. New, compensated carr-purcell sequences. *J Magn Reson* (1969) 89(1990):479–84. doi:10.1016/0022-2364(90)90331-3
  66. Wang ZH, de Lange G, Risté D, Hanson R, Dobrovitski VV. Comparison of dynamical decoupling protocols for a nitrogen-vacancy center in diamond. *Phys Rev B* (2012) 85:479–15. doi:10.1103/PhysRevB.85.155204
  67. Zhao N, Honert J, Schmid B, Klas M, Isoya J, Markham M, et al. Sensing single remote nuclear spins. *Nat Nanotechnol* (2012) 7:657–62. doi:10.1038/nnano.2012.152
  68. Taminiau TH, Wagenaar JJT, van der Sar T, Jelezko F, Dobrovitski VV, Hanson R. Detection and control of individual nuclear spins using a weakly coupled electron spin. *Phys Rev Lett* (2012) 109:137602. doi:10.1103/PhysRevLetters109.137602
  69. Kolkowitz S, Unterreithmeier QP, Bennett SD, Lukin MD. Sensing distant nuclear spins with a single electron spin. *Phys Rev Lett* (2012) 109:137601. doi:10.1103/PhysRevLetters109.137601
  70. Staudacher T, Shi F, Pezzagna S, Meijer J, Du J, Meriles CA, et al. Nuclear magnetic resonance spectroscopy on a (5-nanometer) sample volume. *Science* (2013) 339:561–3. doi:10.1126/science.1231675
  71. Shi F, Zhang Q, Wang P, Sun H, Wang J, Rong X, et al. Single-protein spin resonance spectroscopy under ambient conditions. *Science* (2015) 347:1135–8. doi:10.1126/science.aaa2253
  72. Uhrig GS. Keeping a quantum bit alive by optimized  $\pi$ -pulse sequences. *Phys Rev Lett* (2007) 98:100504. doi:10.1103/PhysRevLetters98.100504
  73. Zhao N, Hu JL, Ho SW, Wan JTK, Liu RB. Atomic-scale magnetometry of distant nuclear spin clusters via nitrogen-vacancy spin in diamond. *Nat Nanotechnol* (2011) 6:242–6. doi:10.1038/nnano.2011.22
  74. Zhao N, Wrachtrup J, Liu RB. Dynamical decoupling design for identifying weakly coupled nuclear spins in a bath. *Phys Rev* (2014) 90:032319. doi:10.1103/PhysRevA.90.032319
  75. Casanova J, Wang ZY, Haase JF, Plenio MB. Robust dynamical decoupling sequences for individual-nuclear-spin addressing. *Phys Rev* (2015) 92:042304. doi:10.1103/PhysRevA.92.042304
  76. Souza AM, Álvarez GA, Suter D. Robust dynamical decoupling for quantum computing and quantum memory. *Phys Rev Lett* (2011) 106:240501. doi:10.1103/PhysRevLetters106.240501
  77. Dreau A, Lesik M, Rondin L, Spinicelli P, Arcizet O, Roch JF, et al. Avoiding power broadening in optically detected magnetic resonance of single nv defects for enhanced dc magnetic field sensitivity. *Phys Rev B* (2011) 84:195204. doi:10.1103/PhysRevB.84.195204
  78. Glaser SJ, Boscain U, Calarco T, Koch CP, Koeckenberger W, Kosloff R, et al. Training Schrödinger's cat: quantum optimal control. *Eur Phys J D* (2015) 69:279. doi:10.1140/epjd/e2015-60464-1
  79. Rembold P, Oshnik N, Müller MM, Montangero S, Calarco T, Neu E. Introduction to quantum optimal control for quantum sensing with nitrogen-vacancy centers in diamond. *AVS Quantum Sci* (2020) 2:024701. doi:10.1116/5.0006785
  80. Häberle T, Schmid-Lorch D, Karrai K, Reinhard F, Wrachtrup J. High-dynamic-range imaging of nanoscale magnetic fields using optimal control of a single qubit. *Phys Rev Lett* (2013) 111:170801. doi:10.1103/PhysRevLetters111.170801
  81. Scheuer J, Kong X, Said RS, Chen J, Kurz A, Marseglia L, et al. Precise qubit control beyond the rotating wave approximation. *New J Phys* (2014) 16:093022. doi:10.1088/1367-2630/16/9/093022
  82. Nöbauer T, Angerer A, Bartels B, Trupke M, Rotter S, Schmiedmayer J, et al. Smooth optimal quantum control for robust solid-state spin magnetometry. *Phys Rev Lett* (2015) 115:190801. doi:10.1103/PhysRevLetters115.190801
  83. Ziem F, Garsi M, Fedder H, Wrachtrup J. Quantitative nanoscale MRI with a wide field of view. *Sci Rep* (2019) 9:12166. doi:10.1038/s41598-019-47084-w
  84. Poggiali F, Cappellaro P, Fabbri N. Measurement of the excited-state transverse hyperfine coupling in nv centers via dynamic nuclear polarization. *Phys Rev B* (2017) 95:195308. doi:10.1103/PhysRevB.95.195308
  85. Goldstein G, Cappellaro P, Maze JR, Hodges JS, Jiang L, Sorensen AS, et al. Environment assisted precision measurement. *Phys Rev Lett* (2011) 106:140502. doi:10.1103/PhysRevLetters106.140502
  86. Hernández-Gómez S, Poggiali F, Cappellaro P, Fabbri N. Quantum control-enhanced sensing and spectroscopy with NV qubits in diamond In: C Soci, MT Sheldon, M Agio, editors *Quantum nanophotonic materials, devices, and systems 2019*. Bellingham, WA, USA: International Society for Optics and Photonics (SPIE) (2019). Vol. 11091, p 31–9. doi:10.1117/12.2531734

87. Bauch E, Hart CA, Schloss JM, Turner MJ, Barry JF, Kehayias P, et al. Ultralong dephasing times in solid-state spin ensembles via quantum control. *Phys Rev X* (2018) 8:031025. doi:10.1103/physrevx.8.031025
88. de Lange G, van der Sar T, Blok M, Wang ZH, Dobrovitski V, Hanson R. Controlling the quantum dynamics of a mesoscopic spin bath in diamond. *Sci Rep* (2012) 2:382. doi:10.1038/srep00382
89. Ekimov E, Kondrin M. Chapter six – high-pressure, high-temperature synthesis and doping of nanodiamonds In: CE Nebel, I Aharonovich, N Mizuochi, M Hatano, editors *Diamond for quantum applications Part 1. Semiconduct semimet*. Cambridge, MA, USA: Elsevier (2020), Vol. 103, p 161–99. doi:10.1016/bs.semsem.2020.03.006
90. Barry JF, Schloss JM, Bauch E, Turner MJ, Hart CA, Pham LM, et al. Sensitivity optimization for nv-diamond magnetometry. *Rev Mod Phys* (2020) 92:015004. doi:10.1103/RevModPhys.92.015004
91. Aharonovich I, Neu E. Diamond nanophotonics. *Adv Opt Mat* (2014) 2: 911–28. doi:10.1002/adom.201400189

**Conflict of Interest:** The authors declare that the research was conducted in the absence of any commercial or financial relationships that could be construed as a potential conflict of interest.

Copyright © 2021 Hernández-Gómez and Fabbri. This is an open-access article distributed under the terms of the Creative Commons Attribution License (CC BY). The use, distribution or reproduction in other forums is permitted, provided the original author(s) and the copyright owner(s) are credited and that the original publication in this journal is cited, in accordance with accepted academic practice. No use, distribution or reproduction is permitted which does not comply with these terms.